

# On the quasi-three dimensional configuration of magnetic clouds

**Q. Hu<sup>1</sup>, W. He<sup>2</sup>, J. Qiu<sup>3</sup>, A. Vourlidas<sup>4,5</sup>, and C. Zhu<sup>3</sup>**

<sup>1</sup>Department of Space Science, and Center for Space Plasma and Aeronomics Research (CSPAR), The University of Alabama in Huntsville, Huntsville, AL 35805, USA

<sup>2</sup>Department of Space Science, The University of Alabama in Huntsville, Huntsville, AL 35805, USA

<sup>3</sup>Physics Department, Montana State University, Bozeman, MT 59717, USA

<sup>4</sup>Johns Hopkins University Applied Physics Laboratory, Laurel, MD 20723, USA

<sup>5</sup>IAASARS, National Observatory of Athens, GR-15236, Penteli, Greece

## Key Points:

- First rigorous applications of a 3D model are carried out for in-situ measurements of MCs
- Results via the optimal fitting approach yield reduced Chi2 values close to 1
- Complexity of MC flux ropes is revealed by the model showing 3D winding magnetic flux bundles

---

Corresponding author: Qiang Hu, [qiang.hu@uah.edu](mailto:qiang.hu@uah.edu)

## Abstract

We develop an optimization approach to model the magnetic field configuration of magnetic clouds, based on a linear-force free formulation in three dimensions. Such a solution, dubbed the Freidberg solution, is kin to the axi-symmetric Lundquist solution, but with more general “helical symmetry”. The merit of our approach is demonstrated via its application to two case studies of in-situ measured magnetic clouds. Both yield results of reduced  $\chi^2 \approx 1$ . Case 1 shows a winding flux rope configuration with one major polarity. Case 2 exhibits a double-helix configuration with two flux bundles winding around each other and rooted on regions of mixed polarities. This study demonstrates the three-dimensional complexity of the magnetic cloud structures.

## Plain Language Summary

Magnetic clouds (MCs) are a type of magnetic field structures observed in space. They possess some well-defined properties and have been well studied in the space age. The existing model for such a structure is a straight cylinder with no variation along its axis. They may impact Earth carrying significant amount of electromagnetic energy. They come in relatively large sizes. When encompassing the near-Earth space environment, their impact can last for days. MCs originate from the Sun, directly born with the so-called coronal mass ejections (CMEs) which can be seen as an ejection of large amount of solar material from telescopes aiming at the Sun. The CMEs are often accompanied by solar flares, the most energetic and explosive events in our solar system. When these happen, they release a wide range of radiations and disturbances that may adversely impact Earth with MCs being one major type of disturbances. Therefore studying the internal configuration of MCs is of importance to understanding their origin and impact. This study presents a more complex MC model to better fit the in-situ spacecraft measurements of such structures, which goes beyond the current model.

## 1 Motivation

Magnetic clouds (MCs) are large-scale magnetic structures (usually with duration  $\gtrsim 1$  day at 1 au) observed from in-situ spacecraft measurements, such as those from the Advanced Composition Explorer (ACE) in the solar wind. MCs possess three well-defined signatures in the magnetic field and plasma measurements: (1) relatively strong total magnetic field, (2) smooth rotation of one or more magnetic field components, and (3)

depressed proton temperature or  $\beta$  value (the ratio between the thermal and magnetic pressures). The elevated magnetic field and low  $\beta$  value often indicate the dominance of the Lorentz force over the plasma pressure gradient and the inertia force for a magnetohydrostatic equilibrium. This leads to the force-free assumption such that the Lorentz force has to vanish. The simplest form, the linear force-free field (LFFF) formulation, has been used to model the magnetic field configuration of MCs. With one-dimensional (1D) dependence on the radial distance  $r$  from a cylindrical axis only, the LFFF model yields the well-known Lundquist solution (Lundquist, 1950), describing an axi-symmetric cylindrical flux rope configuration.

Besides a number of variations to the Lundquist solution (e.g. Farrugia et al., 1999; Nieves-Chinchilla et al., 2016; Wang et al., 2016), which are mostly 1D, a true two-dimensional (2D) model stands out by solving the Grad-Shafranov (GS) equation to obtain a 2D cross section of arbitrary shape of a cylindrical structure based on single-spacecraft measurements (see, Hu, 2017a, for a comprehensive review). This method, so-called GS reconstruction, obtains the magnetic flux function which defines distinct flux surfaces in a 2D configuration, governed by the GS equation. The GS reconstruction was first applied to in-situ observations of magnetic flux ropes by Hu and Sonnerup (2001, 2002); Hu et al. (2003, 2004). The solution yields nested flux surfaces, representing winding magnetic field lines lying on distinct cylindrical surfaces surrounding a central axis.

MCs are always entrained in coronal mass ejections (CMEs), often associated with solar flares. Efforts have been made to relate the MC flux rope configuration with the solar source region properties. For example, we have carried out several investigations of comparing magnetic flux contents and twist profiles in MCs with those derived from flare observations, giving rise to the birth and build-up of the CME flux ropes (Qiu et al., 2007; Hu et al., 2014; Wang et al., 2017, 2019; Zhu et al., 2020). These are largely based on highly quantitative observational analysis, and somewhat simplified 2D considerations. Recently we have compiled additional lists of flare/CME-MC event pairs awaiting further analysis (Zhu et al., 2020). A challenge we are facing is the inadequacy of the flux rope modeling based on in-situ spacecraft measurements. The current models, 2D at best even with the latest developments (see, e.g., Hu, 2017b), may not yield successful fits for all MC events. Numerous observations and numerical studies indicate the three-dimensional (3D) nature of flux rope configurations upon their origination on the Sun (e.g., Vourlidas et al., 2013; Vourlidas, 2014; Amari et al., 2018; Jiang et al., 2016;

Duan et al., 2019), often in the form of twisted ribbons. To bridge this gap, we develop an approach to probe the 3D MC field line configuration from in-situ data. An earlier attempt was made by Osherovich et al. (1999), which showed a double-helix configuration as a solution to an alternative theoretical model, but lacked rigorous applications to in-situ data. In what follows, we demonstrate our approach with optimal fitting of the 3D Freidberg solution (Freidberg, 2014) to single spacecraft measurements of MCs, strictly following the appropriate  $\chi^2$  minimization methodology (Press et al., 2007).

## 2 Method

The method we develop is based on an LFFF formulation in three dimensions, namely, in a cylindrical coordinate system  $(r, \theta, z)$ . The following is a direct copy of the set of equations given in Freidberg (2014), representing a series solution to the equation  $\nabla^2 \mathbf{B} + \mu^2 \mathbf{B} = 0$  with the force-free constant  $\mu$ ,

$$\frac{B_z(r)}{B_{z0}} = J_0(\mu r) + C J_1(\alpha r) \cos(\theta + kz) \quad (1)$$

$$\frac{B_\theta(r)}{B_{z0}} = J_1(\mu r) - \frac{C}{\alpha} \left[ \mu J'_1(\alpha r) + \frac{k}{\alpha r} J_1(\alpha r) \right] \cos(\theta + kz) \quad (2)$$

$$\frac{B_r(r)}{B_{z0}} = -\frac{C}{\alpha} \left[ k J'_1(\alpha r) + \frac{\mu}{\alpha r} J_1(\alpha r) \right] \sin(\theta + kz). \quad (3)$$

Such a solution (dubbed the Freidberg solution) is obtained by truncating the infinite series and keeping the first two modes through a standard separation of variables procedure. For  $C \equiv 0$ , the solution reduces to the axis-symmetric Lundquist solution. Generally the solution has 3D dependence on spatial dimensions, but it is also periodic in  $z$  with a period/wavelength  $2\pi/k$ , thus called a solution of “helical symmetry” with mixed helical states of azimuthal wavenumbers  $m = 0$  and  $1$ . The parameter  $C$  determines the amplitude of the  $m = 1$  mode, which gives rise to the variation in  $\theta$ . Following Freidberg (2014), the LFFF constant is denoted  $\mu$  and the parameter  $\alpha = (\mu^2 - k^2)^{1/2}$ . The usual Bessel’s functions of the first kind of the zeroth and first order are denoted  $J_0$  and  $J_1$ , respectively.

For an MC event detected in in-situ spacecraft data, an interval is chosen for a  $\chi^2$  minimization process to determine the unknown parameters in the Freidberg solution, i.e., equations (1)-(3). A reduced  $\chi^2$  function is defined to assess the difference between the measured magnetic field components  $\mathbf{b}$  and the analytic solution  $\mathbf{B}$ , subject to un-

derlying uncertainties:

$$\chi^2 = \frac{1}{\text{dof}} \sum_{\nu=X,Y,Z} \sum_{i=1}^N \frac{(b_{\nu i} - B_{\nu i})^2}{\sigma_i^2}. \quad (4)$$

A minimum  $\chi^2$  value is sought for an interval with  $N$  magnetic field data points, often downsampled from 1-min cadence to 1 hour. Then the degree of freedom (`dof`) of the system is  $3N - p - 1$ , with  $p$  the number of parameters to be optimized. According to Press et al. (2007), a quantity  $Q$ , indicating the probability of a value greater than the specific  $\chi^2$  value, is also obtained for reference. It is calculated by  $Q = 1 - \text{chi2cdf}(\chi^2, \text{dof})$ , where the function `chi2cdf` is the cumulative distribution function of  $\chi^2$ . The corresponding uncertainties  $\sigma$  are estimated by taking the root-mean-square (RMS) variation of the underlying 1-min measurements over each one-hour interval, an approach adopted by the ACE Science Center MAG data processing (see [http://www.srl.caltech.edu/ACE/ASC/level2/mag\\_12desc.html](http://www.srl.caltech.edu/ACE/ASC/level2/mag_12desc.html)). The set of main parameters to be optimized includes  $C$ ,  $\mu$ ,  $k$ , the pair of the directional angles of the  $z$  axis,  $(\delta, \phi)$ , together with additional geometrical parameters to allow for more freedom of the solution with respect to the space-craft path. Simply put, besides that the  $z$  axis orientation is completely arbitrary, the outer cylinder enclosing the solution domain is allowed to translate along and perpendicular to, as well as to rotate about the  $z$  axis. This fully accounts for the 3D nature of the solution. Detailed descriptions of the algorithm will be reported elsewhere. In the following case studies, the parameters  $\mu$  and  $k$  become dimensionless by multiplying a length scale  $R_0$  which is the normalization constant for  $r$  and  $z$ .

### 3 Case Studies

We present two case studies to illustrate the method. Case 1 is an MC event observed on 14 April 2013 at 1 au. Figure 1 shows the time-series plot from the ACE space-craft measurements. A typical MC structure is present with relatively strong field magnitude and rotating field components, and depressed proton  $\beta$ . Two intervals are marked. Both last for over 20 hours. The average Alfvén Mach number in the reference frame moving with the MC structure is 0.23, and the average  $\beta$  is 0.01, justifying the assumption of quasi-static equilibrium and approximate force-freeness. A GS reconstruction was performed with acceptable output. The optimization result for the Freidberg solution is shown in Figure 2 with the minimum reduced  $\chi^2 = 0.978$ , and  $Q = 0.531$ .

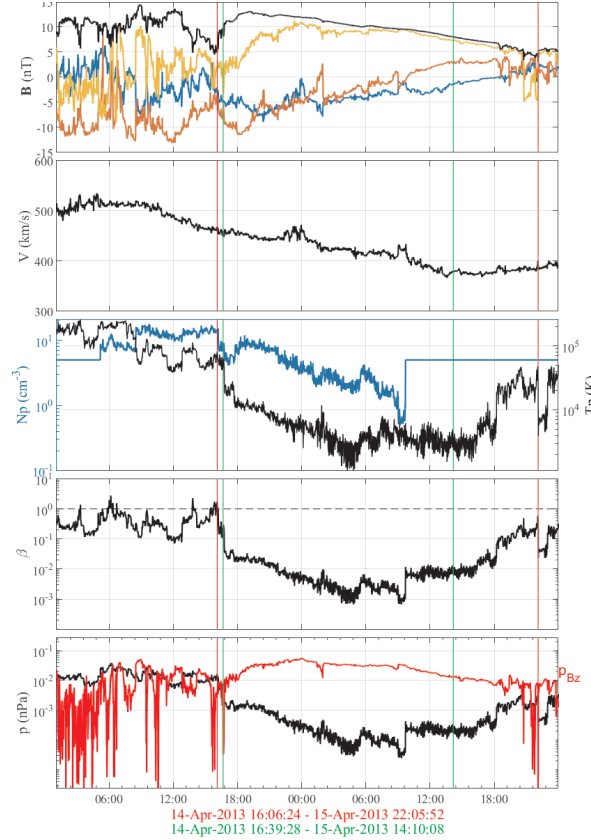


**Figure 1.** Time-series from the ACE spacecraft measurements for Case 1. From top to bottom: magnetic field components in R (blue), T (brown), and N (gold) coordinates, and magnitude (black), bulk speed, proton density (left axis) and temperature (right axis), proton  $\beta$ , and thermal and axial magnetic pressure (red). The vertical lines mark the intervals for the GS reconstruction (green) and the optimization analysis (red) of the Freidberg solution with the corresponding time periods denoted beneath the bottom panel, respectively.

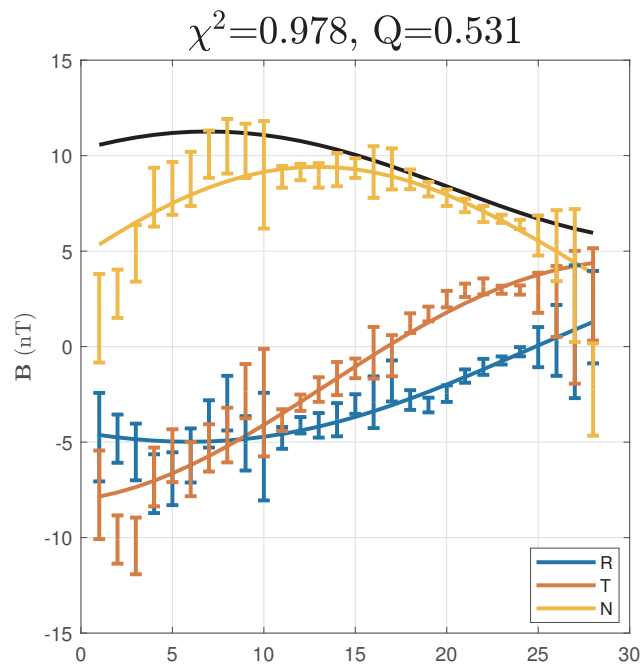
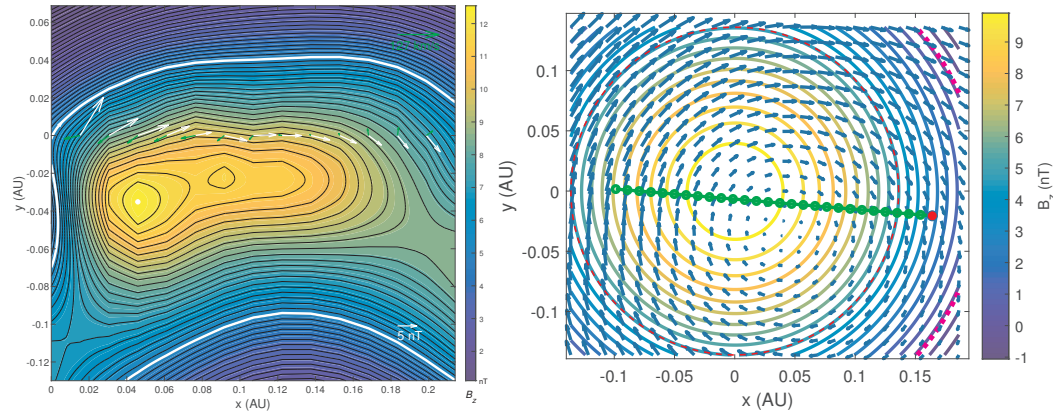


**Figure 2.** The optimal fitting results to the Freidberg solution for Case 1. The error bars are the ACE measurements with uncertainties in hourly averages, and the solid curves are the Freidberg solution, for the R, T, and N components, respectively, as indicated by the legend. The field magnitude is in black.

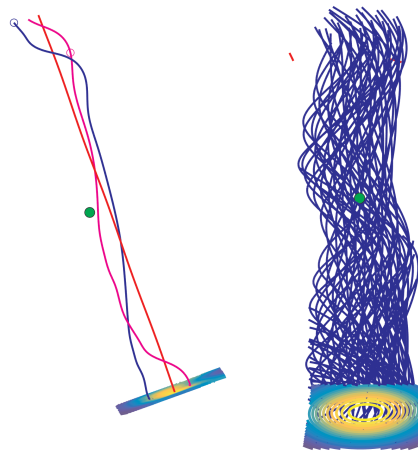
Figures 3 and 4 further demonstrate the similarity, but more pronounced the differences between the two solutions. Figure 3, left panel, shows the cross section of a flux rope from the GS reconstruction in the form of the contour lines of the 2D flux function and the co-spatial axial field. In other words, the solution is fully represented by this 2D rendering in a view down the  $z$  axis of a set of (nested) distinct flux surfaces. It is readily seen that the flux rope configuration is left-handed as indicated by the white arrows and the positive  $B_z$  field along the spacecraft path. On the other hand, the Freidberg solution, given to the right, loses this 2D feature. This is the same view down the  $z$  axis with the cross section drawn at  $z = 0$  where the first point along the spacecraft path is located. Then the spacecraft path (green dots) deviates from this plane. There are no distinct flux surfaces, and such a cross-section plot will change with  $z$ . Both solutions yield a uni-polar region of positive axial field. The axial magnetic flux is  $\Phi_z = 5.7 \times 10^{20}$  Mx, and  $9.6 \times 10^{20}$  Mx, respectively. For the Freidberg solution, the sign of the parameter  $\mu = -1.61$  indicates the negative sign of magnetic helicity, i.e., left-handed chirality. The larger amount of flux in the Freidberg solution is partially due to the corresponding larger interval used for this analysis (see Figure 1).

Figure 4 provides a 3D view of field-line configurations toward the Sun for both solutions. Overall they are similarly oriented in space, with the  $z$  axes pointing mainly northward. The drastic difference, however, not in the number of field lines drawn for each, lies in the intrinsic differences between a 2D and a (quasi-) 3D configuration. In the right panel, more field lines are drawn to illustrate the overall winding of the flux rope body, which is not present in the left panel where the flux rope remains straight.

It is more informative to demonstrate by Case 2 the novelty of the new approach and the complexity of the field configuration represented by the Freidberg solution, whereas the GS reconstruction failed to yield a satisfactory result. Case 2 is a well-studied Sun-Earth connection event with a prolonged MC interval occurring on 15 July 2012. We refer readers to the VarSITI Campaign event webpage ([http://solar.gmu.edu/heliophysics/index.php/07/14/2012\\_17:00:00\\_UTC](http://solar.gmu.edu/heliophysics/index.php/07/14/2012_17:00:00_UTC)) for detailed information and references on relevant studies. An optimal Freidberg solution is obtained over a 27-hour interval, as shown in the left panel of Figure 5. The reduced  $\chi^2$  value is slightly greater than 1. The corresponding set of optimal parameters indicates a more significant helical component and right-handed chirality ( $C = -2.27$ ;  $\mu = 5.64$ ). Indeed, the corresponding 3D field line configuration in Figure 5 shows a striking double-helix structure with two bundles of field



**Figure 3.** The cross sections of the GS reconstruction result (left panel), and the Freidberg solution at  $z = 0$  (right panel) for Case 1. In the left panel, the black contour lines represent the transverse field lines and color represents the axial field with scales indicated by the colorbar. The white (green) arrows along  $y = 0$  are the measured transverse field (remaining transverse flow) vectors along the spacecraft path. A reference vector for each set is shown (where the green reference vector is of the magnitude of the average Alfvén speed). In the right panel, the color contours show the axial field at  $z = 0$ , and the corresponding transverse field is shown by arrows. The dots mark the spacecraft path during the analysis interval in 1 hour increment from start (the leftmost green dot) to the end (the red dot). Note that they are not lying on this plane except for the leftmost dot.



**Figure 4.** The 3D view toward the Sun of the field-line configurations for the GS reconstruction result (left panel), and the Freidberg solution (right panel), for Case 1. The big green dot marks the spacecraft path along the -R direction, the N direction is straight up, and the T direction is horizontally to the right. Both sets of field lines are winding upward out of the bottom plane where contours of  $B_z$  are shown. The  $z$  axis orientations are  $(0.08206, -0.3377, 0.9377)$ , and  $(-0.4706, -0.0350, 0.8817)$ , in RTN coordinates, respectively.

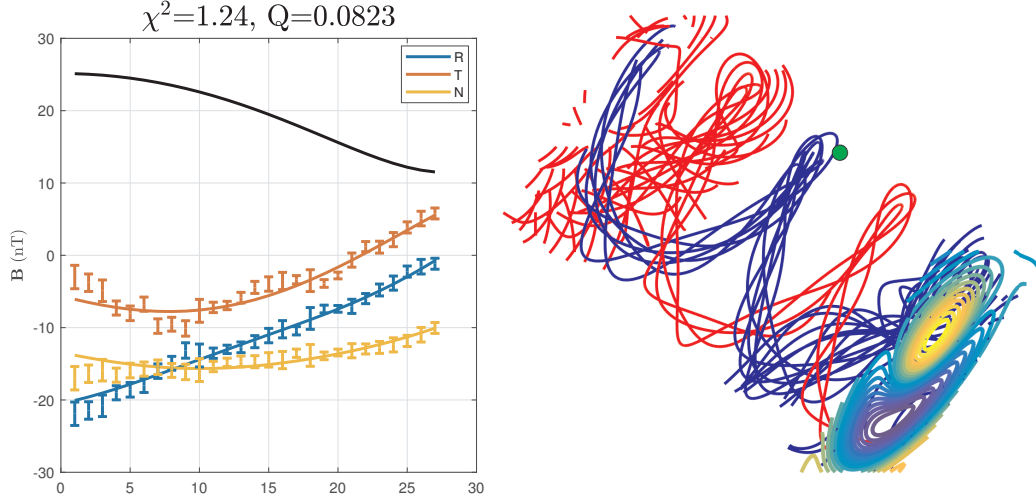


**Figure 5.** Left panel: The optimal fitting result to the Freidberg solution for Case 2.

The format is the same as Figure 2. Right panel: The 3D view toward the Sun of the field-line configuration for the Freidberg solution. The format is the same as Figure 4. The set of red field lines are winding downward into the bottom plane. The  $z$  axis orientation is  $(-0.3265, -0.7509, 0.5741)$  in the RTN coordinates.

lines (blue and red) winding up and down along the  $z$  axis and around each other. The cross section at the bottom clearly shows the mixed  $B_z$  polarity regions next to each other, corresponding to the two flux bundles. Both are right-handed. In this event, the spacecraft is taking a glancing path across such a complex system.

#### 4 Conclusions

In conclusion, we have developed a new approach to model the MC magnetic field in a quasi-3D configuration. The model is based on an LFFF formulation presented in Freidberg (2014), which is a generalization of the well-known Lundquist solution. The solution is 3D in nature as a function of  $(r, \theta, z)$  in a cylindrical coordinate system, but with periodicity in  $z$ . A  $\chi^2$  minimization process is devised by using the in-situ spacecraft measurements with underlying uncertainty estimates to determine the optimal set of parameters that yields a solution with the best fit to the magnetic field vectors along the spacecraft path. Two case studies are presented to illustrate the merit of the methodology. Both results are obtained with minimum reduced  $\chi^2 \approx 1$  and the associated  $Q \gg 10^{-3}$ , deemed acceptable according to Press et al. (2007). Case 1 exhibits a flux rope con-

figuration with certain similarity to the corresponding 2D GS reconstruction result. Their  $z$  axis orientations and the axial magnetic flux contents are similar, and the chirality is the same. However the results are markedly different in that the Fieidberg solution exhibits a more general and intrinsically 3D field configuration with a winding flux rope body. Potentially more complex MC structure is revealed by Case 2 in which a double-helix configuration is obtained. The cross section of the structure contains two adjacent regions of opposite field polarities (so are the currents) where the two helical flux bundles originate, both with right-handed chirality. Such a configuration, originating from the Sun, implies that the footpoint regions must have mixed polarities as well. The ultimate proof of these implications has to come from quantitative comparisons with solar source region properties. This future investigation involving more extensive lists of events with well-coordinated observations will be facilitated by this new tool developed here and will be pursued within our team.

### Acknowledgments

The authors acknowledge NASA grant 80NSSC18K0622 for partial support. In addition, QH acknowledges NASA grants 80NSSC19K0276, 80NSSC17K0016 and NSF grant AGS-1954503 for support. WH and QH acknowledge NSF grant AGS-1650854 and NSO DKIST Ambassador program for support. The ACE spacecraft Level2 data are accessed via the ACE Science Center (<http://www.srl.caltech.edu/ACE/ASC/>).

### References

Amari, T., Canou, A., Aly, J.-J., Delyon, F., & Alauzet, F. (2018, February). Magnetic cage and rope as the key for solar eruptions. *Nature*, 554(7691), 211-215. doi: 10.1038/nature24671

Duan, A., Jiang, C., He, W., Feng, X., Zou, P., & Cui, J. (2019, October). A Study of Pre-flare Solar Coronal Magnetic Fields: Magnetic Flux Ropes. *The Astrophysical Journal*, 884(1), 73. doi: 10.3847/1538-4357/ab3e33

Farrugia, C. J., Janoo, L. A., Torbert, R. B., Quinn, J. M., Ogilvie, K. W., Lepping, R. P., ... Berdichevsky, D. (1999, June). A uniform-twist magnetic flux rope in the solar wind. In S. T. Suess, G. A. Gary, & S. F. Nerney (Eds.), *American institute of physics conference series* (Vol. 471, p. 745-748). doi: 10.1063/1.58724

Freidberg, J. P. (2014). Ideal mhd. In (p. 546-547). Cambridge, UK: Cambridge University Press.

Hu, Q. (2017a, June). The Grad-Shafranov Reconstruction in Twenty Years: 1996 - 2016. *Sci. China Earth Sciences*, *60*, 1466-1494. doi: doi:10.1007/s11430-017-9067-2

Hu, Q. (2017b, September). The Grad-Shafranov Reconstruction of Toroidal Magnetic Flux Ropes: Method Development and Benchmark Studies. *Solar Physics*, *292*, 116. doi: 10.1007/s11207-017-1134-z

Hu, Q., Qiu, J., Dasgupta, B., Khare, A., & Webb, G. M. (2014, September). Structures of Interplanetary Magnetic Flux Ropes and Comparison with Their Solar Sources. *The Astrophysical Journal*, *793*, 53. doi: 10.1088/0004-637X/793/1/53

Hu, Q., Smith, C. W., Ness, N. F., & Skoug, R. M. (2003, April). Double flux-rope magnetic cloud in the solar wind at 1 AU. *Geophysical Research Letters*, *30*, 1385. doi: 10.1029/2002GL016653

Hu, Q., Smith, C. W., Ness, N. F., & Skoug, R. M. (2004, March). Multiple flux-rope magnetic ejecta in the solar wind. *Journal of Geophysical Research: Space Physics*, *109*, 3102. doi: 10.1029/2003JA010101

Hu, Q., & Sonnerup, B. U. Ö. (2001, February). Reconstruction of magnetic flux ropes in the solar wind. *Geophysical Research Letters*, *28*, 467-470. doi: 10.1029/2000GL012232

Hu, Q., & Sonnerup, B. U. Ö. (2002, July). Reconstruction of magnetic clouds in the solar wind: Orientations and configurations. *Journal of Geophysical Research: Space Physics*, *107*, 1142. doi: 10.1029/2001JA000293

Jiang, C., Wu, S. T., Feng, X., & Hu, Q. (2016, May). Data-driven magnetohydrodynamic modelling of a flux-emerging active region leading to solar eruption. *Nature Communications*, *7*, 11522. doi: 10.1038/ncomms11522

Lundquist, S. (1950). On force-free solution. *Ark. Fys.*, *2*, 361.

Nieves-Chinchilla, T., Linton, M. G., Hidalgo, M. A., Vourlidas, A., Savani, N. P., Szabo, A., ... Yu, W. (2016, May). A Circular-cylindrical Flux-rope Analytical Model for Magnetic Clouds. *The Astrophysical Journal*, *823*, 27. doi: 10.3847/0004-637X/823/1/27

Osherovich, V. A., Fainberg, J., & Stone, R. G. (1999, January). Multi-tube model

for interplanetary magnetic clouds. *Geophysical Research Letters*, 26(3), 401-404. doi: 10.1029/1998GL900306

Press, W. H., Teukolsky, S. A., Vetterling, W. T., & Flannery, B. P. (2007). *Numerical Recipes in C++ : The Art of Scientific Computing*. New York: 778, Cambridge Univ. Press. doi: <http://numerical.recipes/>

Qiu, J., Hu, Q., Howard, T. A., & Yurchyshyn, V. B. (2007, April). On the Magnetic Flux Budget in Low-Corona Magnetic Reconnection and Interplanetary Coronal Mass Ejections. *The Astrophysical Journal*, 659, 758-772. doi: 10.1086/512060

Vourlidas, A. (2014, June). The flux rope nature of coronal mass ejections. *Plasma Physics and Controlled Fusion*, 56(6), 064001. doi: 10.1088/0741-3335/56/6/064001

Vourlidas, A., Lynch, B. J., Howard, R. A., & Li, Y. (2013, May). How Many CMEs Have Flux Ropes? Deciphering the Signatures of Shocks, Flux Ropes, and Prominences in Coronagraph Observations of CMEs. *Solar Physics*, 284(1), 179-201. doi: 10.1007/s11207-012-0084-8

Wang, W., Liu, R., Wang, Y., Hu, Q., Shen, C., Jiang, C., & Zhu, C. (2017, November). Buildup of a highly twisted magnetic flux rope during a solar eruption. *Nature Communications*, 8, 1330. doi: 10.1038/s41467-017-01207-x

Wang, W., Zhu, C., Qiu, J., Liu, R., Yang, K. E., & Hu, Q. (2019, January). Evolution of a Magnetic Flux Rope toward Eruption. *The Astrophysical Journal*, 871(1), 25. doi: 10.3847/1538-4357/aaf3ba

Wang, Y., Zhuang, B., Hu, Q., Liu, R., Shen, C., & Chi, Y. (2016). On the twists of interplanetary magnetic flux ropes observed at 1 au. *Journal of Geophysical Research: Space Physics*, 121(10), 9316–9339. Retrieved from <http://dx.doi.org/10.1002/2016JA023075> (2016JA023075) doi: 10.1002/2016JA023075

Zhu, C., Qiu, J., Liewer, P., Vourlidas, A., Spiegel, M., & Hu, Q. (2020, April). How Does Magnetic Reconnection Drive the Early-stage Evolution of Coronal Mass Ejections? *The Astrophysical Journal*, 893(2), 141. doi: 10.3847/1538-4357/ab838a